

# Studies on Semi-Interpenetrating Polymer Network Based on Nitrile Rubber and Poly(Methyl Methacrylate)

A. B. Samui, V. G. Dalvi, M. Patri, B. C. Chakraborty, P. C. Deb

Naval Materials Research Laboratory, Shil-Badlapur Road, Ambernath (E), Thane 421506, India

Received 6 November 2002; accepted 8 April 2003

**ABSTRACT:** Sequential interpenetrating polymer networks (IPNs) based on nitrile rubber and poly(methyl methacrylate) (PMMA) were synthesized. IPN compositions were varied by varying the swelling time. Two methods were adopted for making IPNs. The first method is "single-step IPN" (SIPN) and the second method is "multistep IPN" (MIPN). The compositions were fixed around 90, 80, 70, 60 and 50% of NBR. In SIPN mode, swelling in monomer and subsequent curing was done once. In MIPN mode, swelling in monomer and curing was repeatedly done. Tensile strength of IPNs was found to increase with PMMA content, MIPN showing higher strength compared to SIPN. Dynamic

modulus showed a similar trend. The  $\tan \delta$  value was found to decrease with PMMA content. At 62/38 nitrile rubber (NBR)/PMMA, MIPN composition isolated  $\tan \delta$  peaks appeared near glass transition temperatures of NBR and PMMA, respectively. Scanning electron micrograph showed phase-separated morphology at the same MIPN composition. Solvent resistance increased with IPN formation maintaining higher resistance for MIPN compared to SIPN. © 2003 Wiley Periodicals, Inc. *J Appl Polym Sci* 91: 354–360, 2004

**Key words:** IPNs; morphology; phase separation; rubber

## INTRODUCTION

Interpenetrating polymer networks (IPNs) are a branch of polyblends having interlocking structure without covalent bond between the constituent polymers. These comprise a rather broad area and consequently have many diverse aspects. One of the more useful properties of IPNs is their damping behavior.<sup>1–12</sup> Application of such polymers to vibrating substrates leads to reduction of mechanical vibrations, which minimizes transmitted noise and decreases substrate fatigue. Phase-separated multicomponent polymers exhibit good damping only near the glass transition temperatures ( $T_g$ 's) of the constituent polymers. Limited phase separation caused by the unique microstructure of IPNs broadens the glass transition regions of the component networks and can merge them into a single transition covering a wide temperature range.<sup>13–17</sup> One more important property of IPNs is that there is simultaneous improvement of mechanical strength.

The final phase morphology of IPNs is usually microheterogeneous and depends not only on the chemical nature of the components but also on the synthesis route and the kinetics of network formation. However, Widmaier et al. demonstrated that the morphology of a sequential IPN depends mainly on the average elas-

tic behavior of the preformed network and not its inhomogeneities and chemical structure.<sup>18</sup> The relative rate of the two competing kinetic processes of phase separation and network formation is the most important factor for controlling the morphology of the final product.

We have reported studies on several elastomeric IPNs and have shown that high damping over a wide temperature and frequency range is possible while maintaining high dynamic modulus.<sup>15,19–20</sup> It remains a curiosity whether the property of IPN can be modified by changing the process, while the final composition is kept constant.

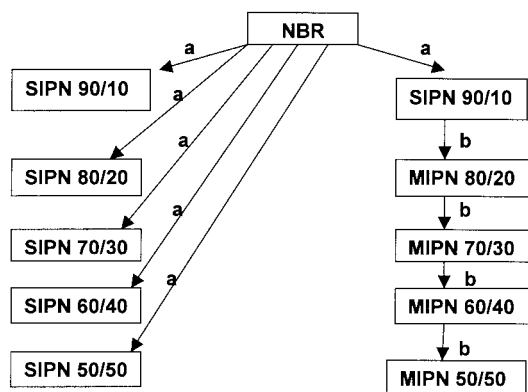
In this article, we report the synthesis of IPNs by both single step (SIPN) as well as multiple step (MIPN) route. The properties of IPNs after each step were measured and an attempt has been made to analyze the difference in behavior of materials made by the two modes.

## EXPERIMENTAL

### Materials

Nitrile rubber (acrylonitrile content: 31%) (NBR), dicumyl peroxide (DCP), obtained from M/s Rubochem Ltd. (India), and tetraethylene glycol dimethacrylate (TEGDM) (Fluka) were used as received. Benzoyl peroxide (BPO; BDH) was recrystallized from methanol prior to use. Methyl methacrylate (MMA) (Fluka) was freed from inhibitor by standard technique.

Correspondence to: P. C. Deb (director@ncml.ernet.in).



- a: Direct swelling of NBR in monomer and curing  
 b: Swelling of already formed IPN in monomer and curing

**Figure 1** Scheme for synthesis of SIPN and MIPN.

## Methods

NBR sheets and IPNs obtained from NBR sheets were prepared by the method described earlier.<sup>15</sup> For making the NBR sheet, it was masticated; then three parts of DCP were mixed in a two-roll mill and the rubber was cured into a sheet form at 150°C for 20 min under a pressure of 50 kg/cm<sup>2</sup> in a compression-molding machine. For making SIPN, a preweighed sheet of cured NBR was swollen in MMA/TEGDM/AIBN (100/0.5/1; w/w). NBR-to-monomer solution weight ratio was maintained at 1 : 20. The swollen NBR sheet was placed between two metal plates and curing was done by heating at 60°C in an air oven for 8 h. The IPN, thus formed, was heated at 50°C under vacuum to constant weight. For making MIPN, previously formed NBR/PMMA IPN was reswelled in MMA/TEGDM/AIBN (100/0.5/1; w/w) mixture for a predetermined period to attain controlled weight increase. Curing of the swelled network was performed by a similar technique as followed above. The detailed scheme of synthesis of SIPN and MIPN is given in Figure 1.

## Characterization

### Swelling study of IPNs

NBR, crosslinked poly(methyl methacrylate) (PMMA), and a few IPNs were swelled in MMA to check the distribution of monomer between two preexisting networks in MIPN. The samples were cut to small pieces and kept in MMA and removed at various time intervals. After wiping out the adhered monomer on the surface, the samples were immediately weighed.

### Tensile/dynamic mechanical properties

Tensile properties, dynamic/loss modulus, and loss tangent measurements were conducted similarly as

described earlier.<sup>15</sup> Tensile strength and elongation at break of IPNs were measured by using a Universal testing machine (Hounsfield) at room temperature at a crosshead speed of 20 mm/min by using dumbbell-shaped specimens, according to ASTM D 638. Dynamic mechanical analysis was performed by using a dynamic mechanical thermal analyzer (Rheometric Scientific). The samples were cut to pieces (16 × 10 × 2 mm) and dynamic mechanical thermal analysis (DMTA) scans were done at 1-Hz frequency at a heating rate of 3°C/min in the temperature range of -40 to +140°C.

## Scanning electron microscopy (SEM)

IPN samples were fractured after cooling in liquid nitrogen. Fractured samples were exposed to the vapor of an aqueous solution of osmium tetroxide (2% w/v) for 4 h for selective staining of the residual double bonds of NBR.<sup>21</sup> Micrographs were taken by employing a scanning electron microscope (Philips, XL-30).

## RESULTS AND DISCUSSION

In the present study, both SIPN and MIPN were synthesized. In the case of SIPN, PMMA content in NBR/PMMA was varied by monomer uptake during swelling. In the case of MIPN, PMMA content was increased stepwise by making IPN of IPN. The weight increase is accompanied by an increase in number of interpenetration. It is in our interest to see the effect of repeated interpenetration on tensile properties, tan  $\delta$ , phase morphology, and solvent swellability.

### Swelling study of IPN

Figure 2 shows the swelling behavior of various IPNs as well as crosslinked NBR and crosslinked PMMA. It is observed that for all the samples swelling increases with time and the difference in swelling extent is minimum at a lower degree of swelling. PMMA swells to maximum extent and is followed by NBR. It is expected that PMMA will swell to a higher degree compared to NBR because of its similar chemical nature. This indicates that MMA will preferentially go to PMMA phase. After IPN formation, the swelling decreases. This is due to the incorporation of more crosslinks. 90/10 SIPN swells more than 70/30 SIPN, similar to the case of 70/30 and 60/40 MIPN. However, the decrease in swelling of MIPN is more pronounced compared to SIPN. This is understandable as the IPN formation of already formed IPN makes the matrix more compact.

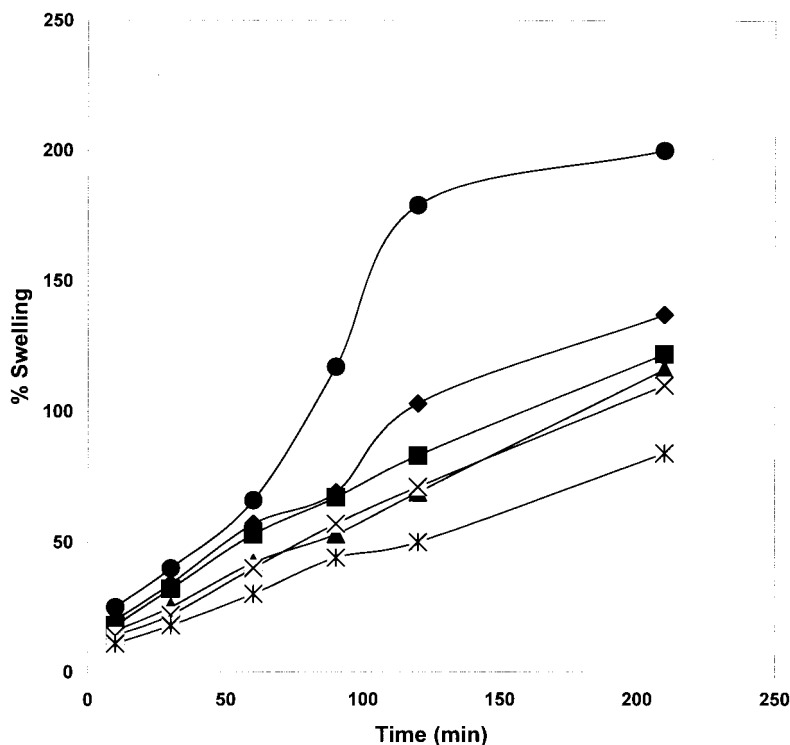


**Figure 2** Variation of swelling with time for NBR, PMMA, SIPN, and MIPN as a function: NBR ( $\blacklozenge$ ); 90/10 SIPN ( $\blacksquare$ ); 70/30 SIPN ( $\blacktriangle$ ); 70/30 MIPN ( $\times$ ); 60/40 MIPN ( $*$ ); PMMA ( $\bullet$ ).

### Tensile properties

Tensile properties are presented in Table I. It can be seen that the tensile strength of pure NBR is low. It increases with PMMA content for both SIPN and MIPN, respectively. The increase is attributed to much higher tensile strength of PMMA. The increase is higher for MIPN than SIPN. In MIPN, the interpenetration is repeated. It is expected that the mechanical strength will be very high because of the further interpenetration of SIPN. However, the values are only

**TABLE I**  
Tensile Properties of IPNs

Samples (NBR/MMA) (w/w)	Tensile strength (MPa)	% Elongation at break
NBR(100/0)	1.45	90
SIPN (89/11)	3.57	86
MIPN	—	—
SIPN (83/17)	4.71	78
MIPN(82/18)	5.65	72
SIPN (68/32)	6.90	73
MIPN(70/30)	6.41	68
SIPN (62/38)	9.20	65
MIPN(62/38)	12.53	42
SIPN (48/52)	16.68	70
MIPN	— <sup>a</sup>	— <sup>a</sup>

<sup>a</sup> Sample is brittle in nature.

marginally higher at lower PMMA content. PMMA is increased in equal amounts in both SIPN and MIPN. The only difference is the mode and extent of crosslinking. As the PMMA content and extent of crosslinking in MIPN are increased, the effect on tensile strength becomes more prominent. It is apparent that PMMA content is the controlling factor at lower MIPN, whereas both PMMA content and extent of crosslinking contribute to the increase of tensile strength at higher MIPN. Values of elongation at break show a decreasing trend as hard PMMA segments are incorporated. The decrease for MIPN is more rapid than that of SIPN. As the interpenetration is done repeatedly, the segmental motion gets more and more restricted. Thus, we can see that at 40% PMMA content in MIPN, the elongation decreases by 50% of original value.

### Dynamic mechanical thermal analysis

Dynamic analysis was carried out in the temperature range of  $-40$  to  $+140^{\circ}\text{C}$ ; the results are summarized in Table II. Figure 3 shows the plot of  $E'$  versus temperature for SIPN. As expected,  $E'$  values increases with PMMA content. This is due to stiffness of PMMA chains. Similar behavior was observed for MIPN. As we can see in Table II, at lower PMMA content, there is not much difference of  $E'$  values of SIPN and MIPN,

TABLE II  
Dynamic Mechanical Properties of NBR and NBR/PMMA IPNs

Sample NBR/PMMA (w/w)	$E'$ at 30°C (MPa)	Temp. for $\tan\delta_{\max}$ (°C)	$\tan\delta_{\max}$ value	$t_a$ (°C)
NBR (100/0)	2.33	-7.1	1.19	26.32
SIPN (89/11)	13.5	-3.1	0.94	27.60
MIPN	—	—	—	—
SIPN (83/17)	19.7	-3.8, 73.7	0.74	26.20
MIPN (82/18)	18.5	-4.3, 87.5	0.69	7.49
SIPN (68/32)	20.1	8.9, 91.4	0.32	23.20
MIPN (70/30)	26.4	-6.2, 74.1	0.30	22.43
SIPN (62/38)	90.2	-3.0, 97.3	0.27	19.18
MIPN (62/38)	117.0	-4.2, 86.1	0.40	15.31
SIPN (48/52)	303	88.3	0.34	24.33
PMMA	1680	92.5	1.35	30.86

respectively. However, with an increase of PMMA, MIPN having a greater number of interpenetration exhibits much higher strength compared to corresponding SIPN. This behavior has also been observed in tensile property measurement. The result indicates that dynamic modulus is mostly dependent on PMMA content at lower PMMA loading. The effect of increasing number of interpenetration becomes prominent at higher PMMA content and at a higher number of interpenetration. Figure 4 shows the  $\tan\delta$  versus temperature plot of NBR-PMMA SIPN. Temperature for  $\tan\delta_{\max}$  and  $t_a$  (area under the curve) values are presented in Table II. NBR shows high  $\tan\delta_{\max}$  at  $-7.1^\circ\text{C}$ .  $\tan\delta_{\max}$  decreases on IPN formation. PMMA content is increased from 0 to 50% (w/w). A high value of  $\tan\delta_{\max}$  for NBR is due to the nitrile group.<sup>22</sup> The contribution of the nitrile group toward  $\tan\delta$

decreases because of the dilution effect by MMA. Crosslinker concentration is maintained at 0.5 wt %. In our earlier study, it was observed that at crosslinker concentration of 2 wt % and above the  $\tan\delta$  peak of NBR/PMMA IPN appeared near the  $T_g$  of NBR.<sup>19</sup> Similar behavior was observed in the present case. After the initial hump, the curve comes down near  $T_g$  of PMMA. However, appreciable  $\tan\delta$  value is maintained over a wide range between  $T_g$  of NBR and PMMA, respectively. As PMMA content is increased,  $\tan\delta$  value near  $T_g$  of PMMA is increased. At 62/38 SIPN composition, the initial hump disappeared and a flat  $\tan\delta$  curve over the entire temperature range is obtained. This seems to be the optimum composition for achieving uniform damping over the entire temperature range. When the PMMA content is increased to 50%, there is a clear hump around  $T_g$  of PMMA. This may be due to the PMMA phase becoming dom-

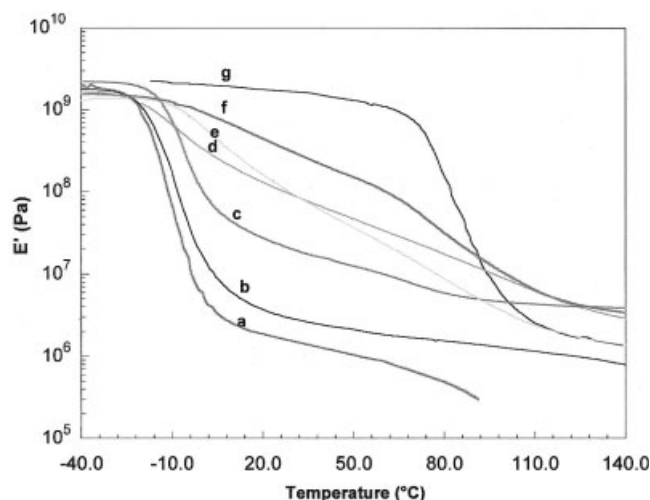


Figure 3 Plots of storage modulus ( $E'$ ) versus temperature of NBR, PMMA, and NBR/PMMA SIPN: (a) NBR; (b) 89 NBR/11 PMMA; (c) 83NBR/17 PMMA; (d) 68 NBR/32 PMMA; (e) 62 NBR/38 PMMA; (f) 48 NBR/52 PMMA; (g) PMMA.

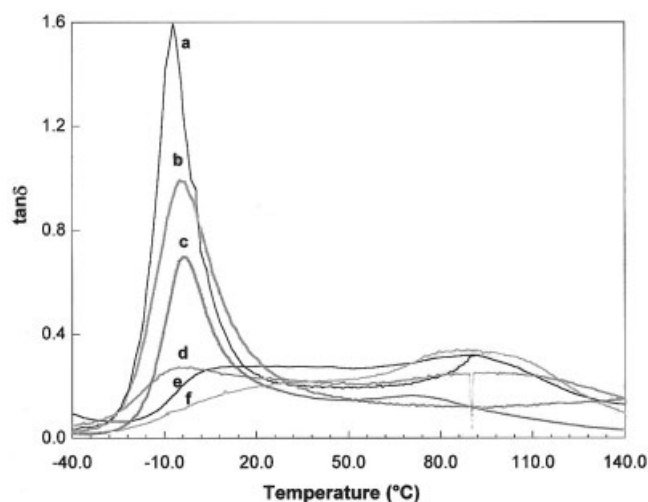
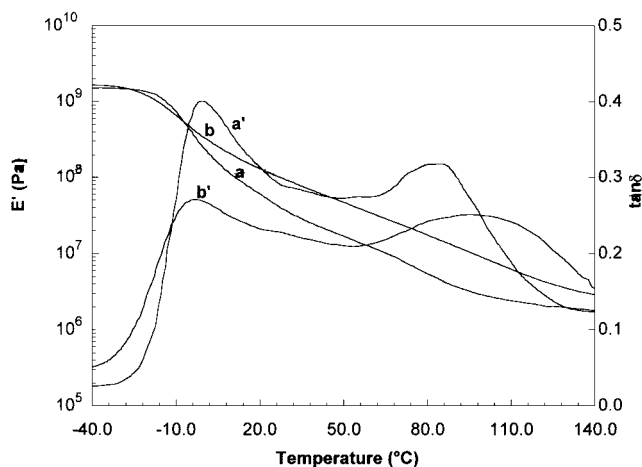


Figure 4 Plots of  $\tan\delta$  versus temperature of NBR and NBR/PMMA SIPN: (a) NBR; (b) 89 NBR/11 PMMA; (c) 83 NBR/17 PMMA; (d) 68 NBR/32 PMMA; (e) 62 NBR/38 PMMA; (f) 48 NBR/52 PMMA.



**Figure 5** Comparison of  $\tan \delta$  and  $E'$  versus temperature plot of 62/38 NBR/PMMA SIPN and MIPN, respectively: (a) and (a') SIPN; (b) and (b') MIPN.

inating. It was not possible to increase PMMA content further because of the brittle nature of the sample. MIPN values are always lower than SIPN values. This is due to the greater number of interpenetrations in MIPN. As the interpenetration number is increased, the segments get more restricted and consequently the loss tangent values show decreasing trend.

Although PMMA content is varied in MIPN, a similar trend, as in the case of SIPN, was observed. However, at 62/38 composition of MIPN, NBR and PMMA peaks appears isolated. Figure 5 describes the comparison of dynamic mechanical properties of SIPN and MIPN, respectively.  $E'$  plots are almost identical. However,  $E'$  values of MIPN around room temperature are lower than that of SIPN.  $\tan \delta$  plots of SIPN and MIPN are completely different. SIPN shows nearly uniform damping, whereas MIPN shows occurrence of phase separation. Two  $\tan \delta$  peaks are observed. The first peak is attributed to the NBR-rich phase around  $-1^\circ\text{C}$  and that of PMMA-rich phase appears around  $86^\circ\text{C}$ . During repeated interpenetration, there is a possibility of some phase being left out or undergoing minimum swelling by monomer, resulting in minimum reinterpenetration. In fact, it has been observed in swelling study that swelling of the crosslinked PMMA phase is higher than that of the NBR phase in MMA. The isolated phases become prominent at 62/38 NBR/PMMA composition. Study on MIPN with further increase of PMMA content was not possible because of the very brittle nature of the sample. Occurrence of clear phase separation indicates that graded damping material can be made by repeated interpenetration method, which will show reasonable damping at a specific temperature and frequency. The area under  $\tan \delta$  temperature curve ( $t_a$ ), which gives an indication about extent of damping, is found to be highest for NBR. On IPN formation, it

decreases. There is no clear trend in the present case. This may be due to the fact that  $\tan \delta$  depends on  $E'$  and  $E''$  and these quantities are different for different IPNs. However, in most of the cases,  $t_a$  values of MIPN are lower than SIPN for obvious reasons.

### Scanning electron microscopy

Figure 6 shows representative micrographs of SIPN and MIPN, respectively. It can be seen that SIPN of 83/17 and 62/38 compositions (a and b) shows uniform distribution of both the phases. Domain sizes were found to be in the range of 80–200 nm. MIPN of 82/18 composition (c) also shows similar uniform distribution of phases. However, a micrograph of 62/38 MIPN (d) appears different from corresponding SIPN. There seems to be partial segregation of one phase at some locations. At other places, the uniformity of phase distribution is maintained. This can be attributed to phase separation of already interpenetrated matrix. At lower PMMA content, the phases remain uniformly distributed for both SIPN and MIPN, respectively. Increasing PMMA does not disturb the distribution pattern. However, at 62/38 composition of MIPN, the uniformity in phases is partially lost. It has already been observed in DMTA studies that a clear peak isolates around  $T_g$  of NBR. As has already been explained, this can be attributed to preferential swelling of one phase in interpenetrated matrix during further swelling by monomer.

### Solvent resistance

Solvent resistance characteristics of NBR and NBR/PMMA IPNs are incorporated in Table III. As expected, the swelling values decrease sharply on incorporation of crosslinked PMMA. With increasing crosslinked PMMA, the swelling values decrease further for SIPN. Swelling of MIPN also decreases similarly. It can be noticed that swelling of SIPN is always lower than that of corresponding MIPN. It is obvious that MIPN, having a higher degree of interpenetration, will offer more resistance to swelling. However, except in one case, no large difference in swelling value was observed.

### CONCLUSION

A series of IPNs based on NBR and PMMA has been synthesized by using single-step and multistep methods routes. The compositions were kept identical in both of the cases. At the same composition of SIPN and MIPN, there is a difference in the number of interpenetration. Tensile measurements, dynamic mechanical thermal analysis, and solvent resistance study were carried out to characterize the IPNs. Tensile strength increased with PMMA content. The effect of

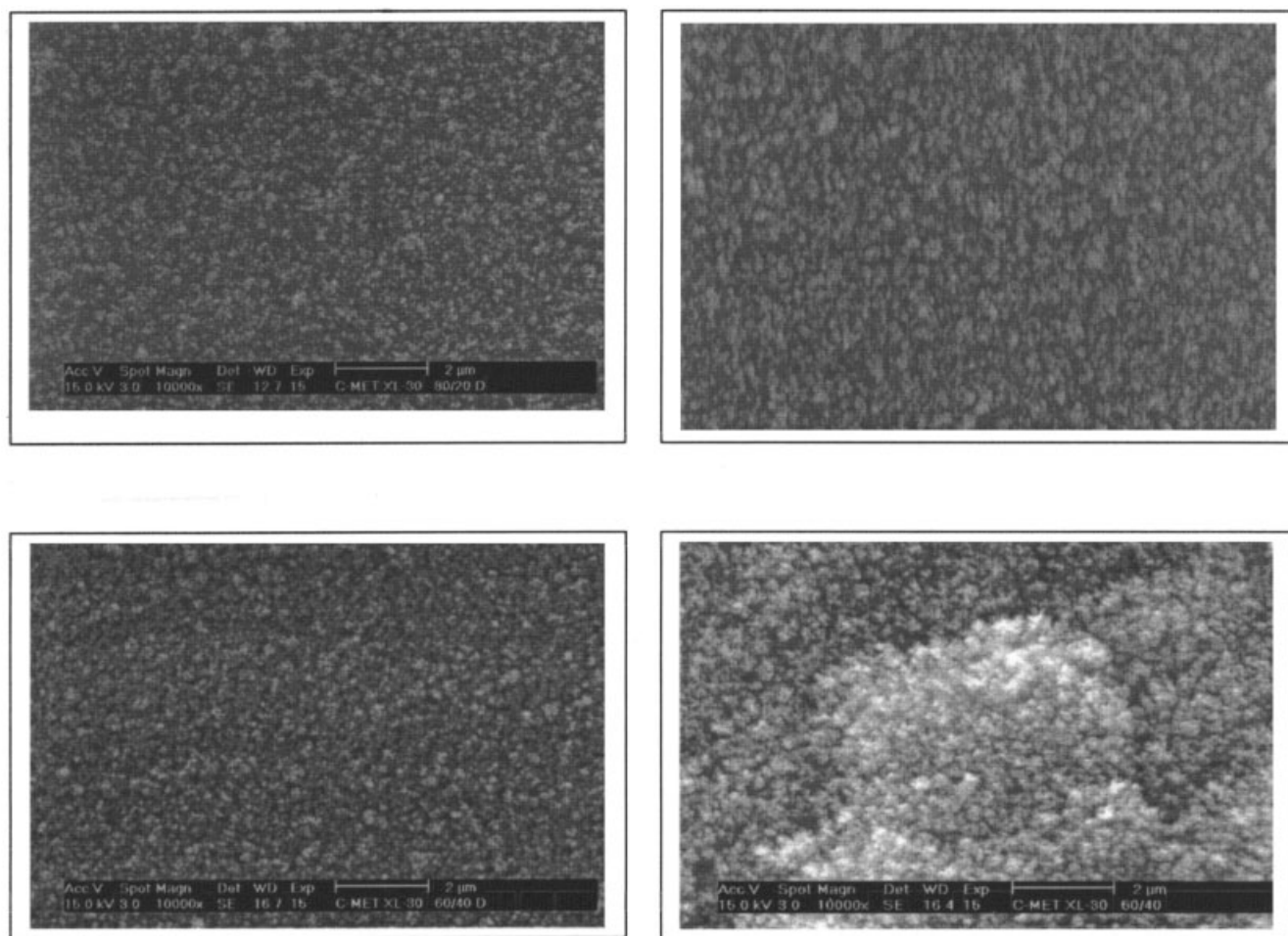


**Figure 6** SEM micrographs of NBR-PMMA IPNs synthesized by single-step (SIPN) and multistep modes: (a) 83/17 SIPN; (b) 82/18 MIPN; (c) 62/38 SIPN; (d) 62/38 MIPN.

repeated interpenetration of MIPN became prominent as the number of interpenetration increased. Tensile strength of MIPN is higher than corresponding SIPN. The difference of tensile strength between SIPN and MIPN increases rapidly with increasing interpenetration at higher PMMA content. Dynamic modulus val-

ues showed a similar trend;  $\tan \delta$  values decreased with introduction of PMMA. Because of the higher number of interpenetration in MIPN, segmental motions were further restricted and are reflected in  $\tan \delta$  values that are lower than that of SIPN. At 62/38 NBR/PMMA MIPN, the  $\tan \delta$  curve showed isolation of peaks around  $T_g$  of NBR and PMMA, respectively. It appeared that there is isolation of some component(s) during repeated swelling in monomer and subsequent curing. It indicates that graded damping can be achieved by using a combination of two or more monomers via the MIPN route. Phase separation was also observed in SEM micrographs. Isolated phases were found to be embedded in a continuous matrix. Solvent resistance was found to be improved after IPN formation. MIPN has shown marginally better resistance compared to SIPN. In conclusion, it can be stated that detailed study with MIPN may lead to a variety of products having distinctly different properties than SIPN. A separate study will be performed at various monomer/crosslinker compositions.

**TABLE III**  
**Results of Swelling Values of IPNs in Various Solvents**

Samples (NBR/MMA) (w/w)	% swelling in				
	Xylene	MIBK	CCl <sub>4</sub>	Ethyl acetate	Engine oil
NBR (100/0)	151	165	142	170	0
SIPN (89/11)	100	123	124	112	0
SIPN (83/17)	95	118	112	102	0
MIPN (82/18)	93	110	108	100	0
SIPN (68/32)	92	107	105	97	0
MIPN (70/30)	86	103	80	92	0
SIPN (62/38)	90	103	100	93	0
MIPN (62/38)	80	90	40	83	0
SIPN (48/52)	74	83	34	75	0

## References

1. Sperling, L. H. *Interpenetrating Polymer Networks and Related Materials*; Plenum Press: New York, 1981.
2. Thomas, D. A.; Sperling, L. H. *Polymer Blends*, Vol. 2; Paul, D. R.; Newman, Eds.; Academic Press: New York, 1978.
3. Frish, H. L.; Frish, K. C.; Klemperer, D. *Pure Appl Chem* 1981, 53, 1557.
4. Hourston, D. L.; McClusky, J. A. *J Appl Polym Sci* 1979, 20, 1573.
5. Foster, J. N.; Sperling, L. H.; Thomas, D. A. *J Appl Polym Sci* 1987, 33, 2637.
6. Hourston, D. J.; Zia, Y. *J Appl Polym Sci* 1983, 28, 2139, 2749, 3849; 1984, 29, 629.
7. Chang, M. C. O.; Thomas, D. A.; Sperling, L. H. *J Appl Polym Sci* 1987, 34, 409.
8. Fox, R. B.; Binter, J. L.; Hinkle, J. H.; Carter, W. *Polym Eng Sci* 1987, 25, 157.
9. Fradkin, D. G.; Foster, J. N.; Sperling, L. H. *Rubber Chem Tech* 1986, 59, 255.
10. Hourston, D. J.; Zia, Y. *Polymer* 1979, 20, 1497, 1573.
11. Wang, D. T. H.; Williams, H. L. *J Appl Polym Sci* 1983, 28, 2187.
12. Hur, T.; Manson, J. A.; Hertzberg, R. W. *Polym Mater Sci Eng* 1987, 56, 273.
13. Ghosh, P.; Ray, P. *J Mater Sci* 1991, 26, 6104.
14. Fay, J. J.; Murphy, C. J.; Thomas, D. A.; Sperling, L. H. *Polym Eng Sci* 1991, 31, 1731.
15. Patri, M.; Samui, A. B.; Deb, P. C. *J Appl Polym Sci* 1993, 48, 1709.
16. Mathew, A.; Chakraborty, B. C.; Deb, P. C. *J Appl Polym Sci* 1994, 53, 1107.
17. Klemperer, D.; Sperling, L. H.; Utracki, L. A., Eds.; *Interpenetrating Polymer Networks*; *Advances in Chemistry Series 239*; American Chemical Society: Washington, DC, 1994.
18. Widmaier, J. M.; Tabka, M. T. *Eur Polym J* 1992, 28 (3), 499.
19. Patri, M.; Samui, A. B.; Chakraborty, B. C.; Deb, P. C. *J Appl Polym Sci* 1997, 65, 549.
20. Samui, A. B.; Suryavanshi, U. G.; Patri, M.; Chakraborty, B. C.; Deb, P. C. *J Appl Polym Sci* 1998, 68, 255.
21. Kato, K. *Polym Eng Sci* 1967, 7, 38.
22. Chang, M. C. O.; Thomas, D. A.; Sperling, L. H. *J Polym Mater* 1989, 6, 61.